Cell Prolif. 2007, **40**, 397–410

BubR1 deficiency results in enhanced activation of MEK and ERKs upon microtubule stresses

Y. L. Yang*, Q. Duan*, T. B. Guo†, X. X. Wang**, Q. Ruan¶, G. T. Xu*, J. W. Zhang*, Z. Y. Lu†, M. Xu*,‡, L. Lu*,§ and W. Dai*,**

**Institute of Health Sciences, Shanghai Institutes for Biological Sciences, Chinese Academy of Sciences, Shanghai, China*, †*Department of Medical Genetics, Shanghai Jiatong University, Shanghai, China*, ‡*Department of Cell Biology Neurobiology and Anatomy, University of Cincinnati College of Medicine, Cincinnati, OH, USA*, §*Division of Molecular Medicine, Harbor-UCLA Medical Center, David Geffen School of Medicine, University of California Los Angeles, Torrance, CA, USA*, ¶*Regeneron Pharmaceuticals Inc., Tarrytown, NY, USA and* ***Department of Environmental Medicine, New York University School of Medicine, Tuxedo, NY, USA*

Received 6 *November* 2006*; revision accepted* 30 *January* 2007

Abstract. Disruption of microtubules activates the spindle checkpoint, of which *BubR1* is a major component. Our early studies show that *BubR1* haplo-insufficiency results in enhanced mitotic slippage *in vitro* and tumorigenesis *in vivo*. *Objective*: Given that both MAPKs/ERKs and MEK play an important role during mitosis, we investigated whether there existed regulatory relationship between the MAPK signalling pathway and *BubR1*. *Method and Results*: Here, we have demonstrated that *BubR1* deficiency is correlated with enhanced activation of MEK and ERKs after disruption of microtubule dynamics. Specifically, treatment with nocodazole and paclitaxel resulted in hyper-activation of ERKs and MEK in $BubR1^{+/-}$ murine embryonic fibroblasts (MEF) compared to that of wild-type MEFs. This enhanced activation of ERKs and MEK was at least partly responsible for more successful proliferation completion when cells were treated with nocodazole. *BubR1* knockdown *via* RNAi resulted in enhanced activation of ERKs and MEK in HeLa cells, correlating with inhibition of PP1, a negative regulator of MEK. Moreover, when *BubR1* was partially inactivated due to premature missegregation of chromosomes after Sgo1 depletion, phosphorylation of ERKs and MEK was enhanced in mitotic cells; in contrast, little, if any activated ERKs and MEK were detected in mitotic cells induced by nocodazole. Furthermore, *BubR1*, activated ERKs and activated MEK all localized to spindle poles during mitosis, and also, the proteins physically interacted with each other. *Conclusion*: Our studies suggest that there exists a cross-talk between spindle checkpoint components and ERKs and MEK and that *BubR1* may play an important role in mediating the cross-talk.

Correspondence: W. Dai, Division of Molecular Carcinogenesis, Department of Medicine, New York Medical College, Basic Science Building, Valhalla, NY 10595, USA. Tel.: 845 731 3555; Fax: 845 731 3611; E-mail: wei.dai@med.nyu.edu. L. Lu, Tel.: 310 787 6853, E-mail: llu@labiomed.org. M. Xu, Tel. 773 834 7937, E-mail: mxu@dacc.uchicago.edu.

INTRODUCTION

The spindle checkpoint, also known as the spindle assembly or the mitotic checkpoint, ensures that cells with defective spindles or defective spindle–kinetochore interactions do not enter anaphase during mitosis. *BubR1* is a key molecule mediating spindle checkpoint activation, during which it is extensively phosphorylated (Chan *et al*. 1999). Loss of spindle checkpoint function inevitably results in chromosomal instability and aneuploidy (Lengauer 2003; Bharadwaj & Yu 2004). Given that aneuploidy is prevalent in many types of cancer, it is believed that spindle checkpoint impairment may be at least partly responsible for loss of control of cell proliferation in the development of malignancy (Lengauer *et al*. 1998). Mutations in *BubR1* have been detected in colonic cancer cells (Cahill *et al*. 1998). Our mouse genetic studies show that haploinsufficiency of *BubR1* results in enhanced genomic instability and development cancer in lung and colon (Dai *et al*. 2004; Rao *et al*. 2005). Consistently, a recent study shows that a defective *BubR1* activity due to specific germline mutations causes aneuploidy, infertility and early onset of malignancies (Hanks *et al*. 2004), strongly suggesting that spindle checkpoint failure is an underlying cause for the development of certain diseases.

The Raf/MEK/MAPK axis is a major molecular pathway regulating cell proliferation (Roovers & Assoian 2000). MEK and MAPKs/ERKs also participate in the regulation of mitosis and meiosis (Castro *et al*. 2001). Zecevic *et al*. (1998) demonstrated that activated ERKs are present at kinetochores, spindle poles and the midbody during mitosis. In NIH3T3 and PtK1 cells, both ERK and MEK are activated during early mitosis, activated ERKs and MEK are localized to spindle poles between prophase and anaphase, and to the midbody during cytokinesis (Shapiro *et al*. 1998). We have also shown that activated ERKs and MEK exhibit spindle localization during prophase and metaphase and that whereas a significant amount of activated ERK remains at spindle poles during telophase, active MEK is primarily localized at the midbody region (Xie *et al*. 2004). ERKs and MEK are essential for mitotic spindle formation and meiotic processes in *Xenopus* oocytes (Castro *et al*. 2001). Verlhac *et al*. have shown that the activity of ERKs significantly increased after rat oocytes entered metaphase and that this increase was correlated with their localization to the spindle poles as revealed by immunofluorescence staining (Verlhac *et al*. 2000). To understand molecular mechanisms controlling the meiotic cell cycle, Tong *et al*. (2003) demonstrated that following treatment with U0126, a specific MEK inhibitor, mouse oocytes contained only one spindle pole, which exhibited an elongated phenotype, suggesting that MEK participated in the formation and maintenance of spindle structures during meiosis.

Active MAPKs are kinetochore components (Zecevic *et al*. 1998) and are implicated in spindle checkpoint activation (Minshull *et al*. 1994). MAPKs interact with and phosphorylate kinetochore motor protein CENP-E, although the physiological relevance of CENP-E phosphorylation remains to be determined (Zecevic *et al*. 1998). MAPKs contribute to cdc20 phosphorylation, which results in its inhibition through binding with other checkpoint proteins such as *BubR1*, Bub3 and Mad2 (Chung & Chen 2003). MAPKs also directly phosphorylate Bub1, and this phosphorylation is associated with its activation in *Xenopus* oocytes (Chen 2004). In addition, *BubR1*, a protein kinase sharing a structural homology with Bub1 and facilitating kinetochore localization of key checkpoint proteins such as Mad1, Mad2, Bub1, Bub3 and CENP-E, appears to be phosphorylated in a MAPK-dependent manner during spindle checkpoint activation (Chen 2004).

Despite that MEK and ERKs or their family members are known to play an active role during cell division and in phosphorylation of components of the spindle checkpoint pathway (Zecevic *et al*. 1998; Chung & Chen 2003; Chen 2004), it remains unclear whether *BubR1* modulates the

activation of major components of the MAPK signalling pathway, especially during mitosis. In this report, we demonstrate that haplo-insufficiency of *BubR1* or its knockdown resulted in hyperactivation of MEK and ERKs, which was correlated with a better cell survival rate in response to microtubule stresses. ERKs, MEK and *BubR1* shared common spindle pole localization during metaphase and were present in the same macromolecular complex, suggesting that these molecules may regulate each other during mitotic progression.

MATERIALS AND METHODS

Murine embryonic fibroblast cells

Primary *BubR1*$^{+/-}$ and wild-type murine embryonic fibroblast (MEF) cells were derived from embryonic day 14.5 (E14.5) embryos produced from *BubR1*$^{+/-}$ intercrosses. MEF cells were cultured under 5% CO_2 in Dulbecco's minimal essential medium supplemented with 0.1 mM β-mercaptoethanol, 15% foetal bovine serum and antibiotics (100 μg/ml penicillin, 50 μg/ml streptomycin sulphate).

Indirect immunofluorescence

Immunofluoresence preparation for microscopy was essentially as described (Wang *et al*. 2002). Briefly, cells were fixed in paraformaldehyde and then were treated with 0.1% Triton X-100. After washing three times with phosphate-buffered saline, cells were blocked in 2.0% bovine serum albumin for 15 min on ice and were incubated with antibodies to phopshorylated ERKs, phosphorylated MEK (Cell Signalling, Danvers, MA, USA), *BubR1* or γ-tubulin for 1 h. After additional washing with phosphate-buffered saline, the cells were incubated with appropriate secondary antibodies conjugated with fluorescein or rhodamine (Jackson Immuno-Research, West Grove, PA, USA) at 4 °C for 1 h in the dark. Cells were then briefly (5 min) stained with 4′,6-diamidino-2-phenylindole (DAPI, Fluka, Buche, Switzerland). Fluorescence microscopy was performed using a Nikon microscope and images were captured using a digital photography (Optronics, Fort Gibson , OK, USA) using Optronics MagFire, Image-Pro Plus software.

Western blotting

Culture medium from MEF cells or HeLa cells was quickly aspirated and the cells were exposed to nocodazole (0.5 μg/ml unless otherwise specified) or paclitaxel (10 nM unless otherwise specified) in fresh medium for a variety of intervals. Treated cells were collected for cell lysate preparation. MEFs or HeLa cells were lysed in lysis buffer as described (Ouyang *et al*. 1997) and equal amounts of cell lysates were subjected to sodium dodecyl sulfate-polyacrylamide gel electrophoresis (SDS-PAGE) followed by immunoblotting analysis with antibodies to *BubR1*, Plk1 (Zymed), ERKs (Cell Signalling), MEK (Cell Signalling), cyclin B1 (Santa Cruz) or β-actin (Cell Signalling). The same lysates were also blotted for phosphorylated ERKs (Cell Signalling), phosphorylated MEK (Cell Signalling), phosphorylated Cdk1 (tyrosine-15, Cell Signalling) or phosphorylated PP1α (threonine-320, Cell Signalling). Specific signals were detected by horseradish peroxidase-conjugated goat antirabbit secondary antibodies (Sigma, St. Louis, MO, USA) and were enhanced using chemiluminescence reagents (Amersham Pharmacia Biotech, Piscataway, NJ, USA).

Cell viability/survival assay

Cell viability was assayed by the 3-(4, 5-dimethylthiazol-2-yl)-2,5-diphenyltetrazolium bromide (MTT) assay method. MEF cells (5×10^3 cells/well) were seeded in a 96-well plate in sextuplicates.

Following 24-h serum starvation that synchronized cells at G_1 phase, each culture well was replaced with fresh growth medium containing foetal bovine serum (10%) and a variety concentrations of nocodazole or paclitaxel. After 24 h culture, MTT (15 μl) was supplied to each well. After incubation at 37 °C for additional 4 h, the medium was removed. MTT formazan precipitates were dissolved in 100 μl SDS/dimethylformamide solution for at least 1 h at 37 °C. Optical density of dissolved samples was measured at 570 nm using a plate reader. For cell survival assays, various cells were exposed to different concentrations of nocodazole or paclitaxel and then were cultured for 24 h before MTT was added.

RNA interference

Double stranded RNAs 21 nucleotides in length were synthesized by Dharmacon Research (Boulder, CO, USA). The targeting sequence of *BubR1* was 5′-AAGGGAAGCCGAGCUGUUGAC-3′, corresponding to the coding region of 1281–1301 in human *BubR1 (*accession no. AF068760) relative to the first nucleotide of ATG start codon. The targeting sequences of *Sgo1* corresponded to the following sequences: 5′-CAUCUUAGCCUGAAGGAUAUU-3′, 5′-UGAAAGAAGCC-CAAGAUAUUU-3′, 5′-CAGCCAGCGUGAACUAUAAUU-3′ and 5′-AAA CGCAGGUCUU-UUAUAGUU-3′. Control siRNA targets luciferase mRNA (accession no. X65324) of the firefly (*Photinus pyralis*), the targeting sequence being 5′-UUCCTACGCTGAGTACTTCGA-3′ (GL-3, Dharmacon Research). RNA duplexes were transfected into HeLa cells *via* the Lipofectamine 2000 approach (Invitrogen). Cells transfected with *BubR1* or luciferase siRNAs for 2 days were treated with nocodazole. Fifteen minutes after nocodazole treatment, the cells were collected and were lysed; equal amounts of cell lysates were used for immunoblotting. Cells transfected with *Sgo1* or luciferase siRNAs for 24 h were collected for cell lysis.

Pull-down assay and co-immunoprecipitation

Recombinant His_6-*BubR1* expressed with the use of a baculoviral expression system as previously described was affinity purified with and subsequently conjugated to Ni-NTA resin (Qiagen, Chatsworth, CA, USA). His_6-*BubR1* resin and control resin were incubated with HeLa cell lysates (1 mg) overnight with gentle rocking at 4 °C. Resin was collected by centrifugation and was rinsed 10 times with cell lysis buffer. Proteins specifically interacting with the resin were analysed by SDS-PAGE followed by Western blotting using antibodies against ERKs and MEKs. For co-immunoprecipitation, equal amounts of HeLa cell lysates were incubated with the *BubR1* antibody or rabbit control immunoglobulin G (IgG) overnight. After thorough washing, immunoprecipitates collected by addition of protein A/G beads were blotted for MEK1. Likewise, HeLa cell lysates were immunoprecipitated with phospho-MEK IgG or rabbit control IgG overnight. MEK immunoprecipitates were blotted for *BubR1*.

RESULTS

It is well known that MEK and MAPKs are important signalling components mediating cell proliferation. However, the exact mechanism by which these kinases directly control mitosis remains rather unclear. Because activated MEK and ERKs are localized to spindle poles and to kinetochores (Shapiro *et al*. 1998) and also are associated with microtubules (Reszka *et al*. 1995), we asked whether a defective spindle checkpoint due to *BubR1*-deficiency would affect activation of MEK and ERKs. Haplo-insufficient *BubR1* MEF cells were established from *BubR1*$^{+/-}$ mice. These cells were genotyped using a strategy as described (Arnaoutov & Dasso

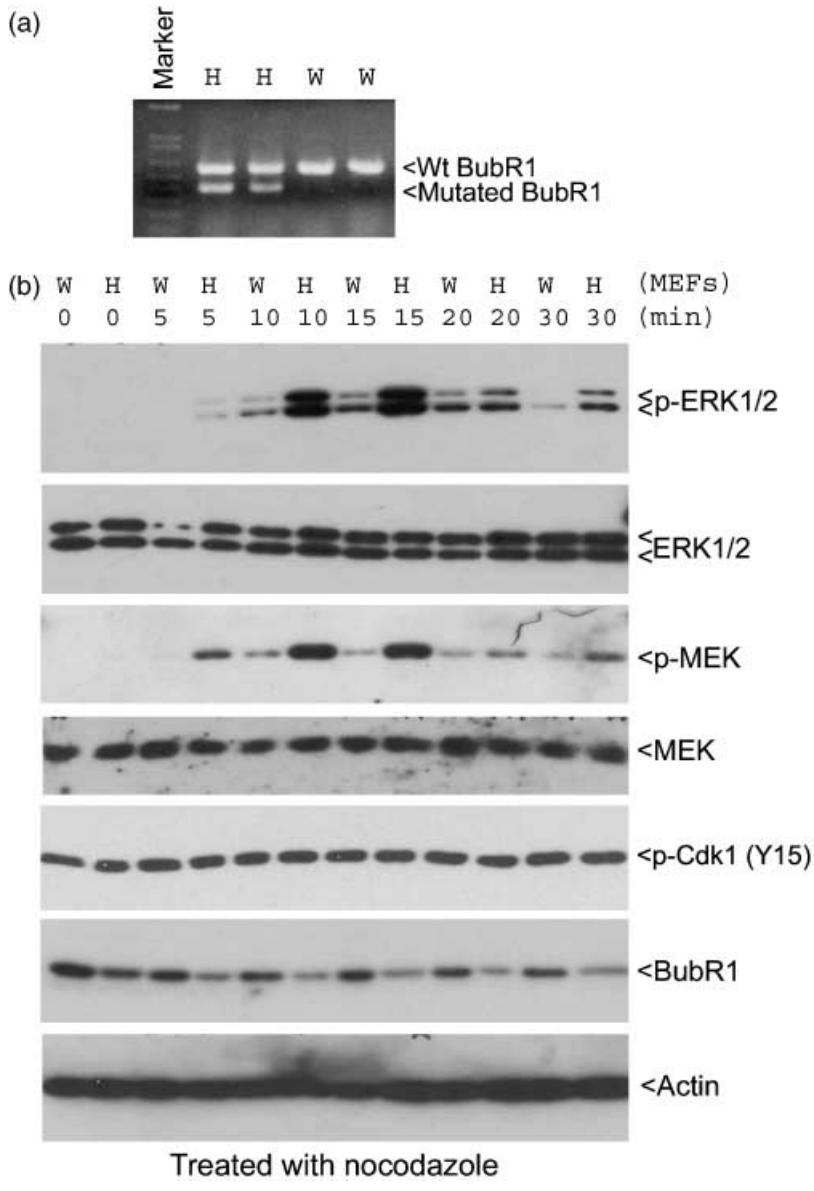

Figure 1. ***BubR1*** **deficiency results in hyper-phosphorylation of ERKs and MEK after nocodazole treatment.** (a) *BubR1*$^{+/-}$ (mutated) and wild-type (Wt) murine embryonic fibroblast (MEF) cells were genotyped via PCR. The PCR products were analysed by agarose gel electrophoresis. (b) *BubR1*$^{+/-}$ (H, heterozygous) and wild-type (W, wild-type) MEF cells were treated with nocodazole for various lengths of time. Equal amounts of protein lysates prepared from the treated cells were immuno-blotted for phosphorylated ERKs, total ERKs, phospho-MEK, total MEK, phosphorylated Cdk1 (Y15), *BubR1* and β-actin.

2003); typical results are shown in Fig. 1(a). Paired MEF cells treated with nocodazole at various times were analysed for activated/phosphorylated ERKs. Little, if any, activated ERKs were detected in untreated MEF cells of either genotype (Fig. 1b). Nocodazole treatment activated ERKs in both wild-type and *BubR1*$^{+/-}$ MEFs. However, ERK activation was more pronounced

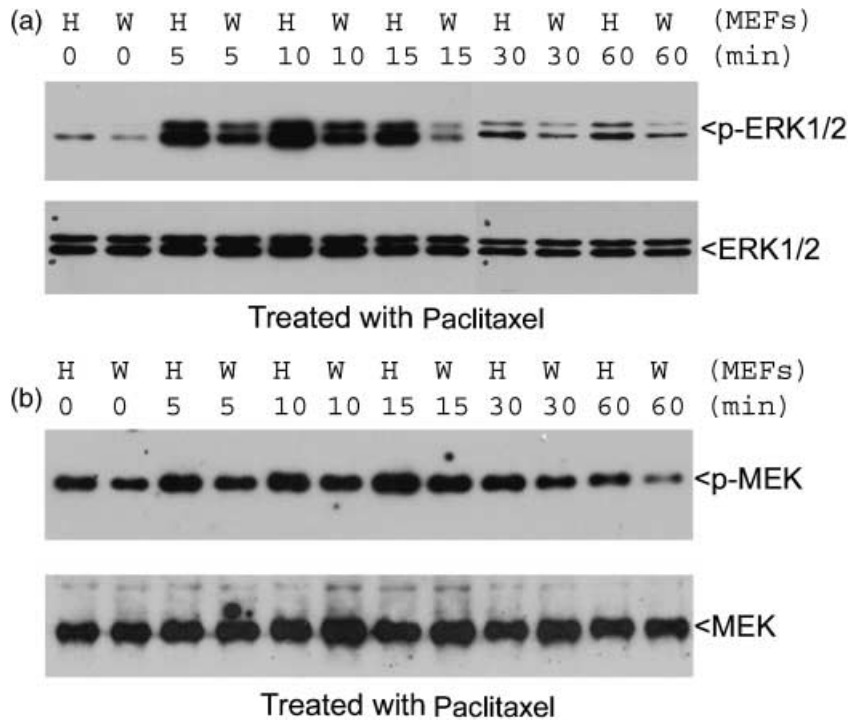

Figure 2. *BubR1* deficiency results in hyper-phosphorylation of ERKs and MEK after paclitaxel treatment. *BubR1*$^{+/-}$ (H, heterozygous) and wild-type murine embryonic fibroblast (MEF) (W, wild-type) cells were treated with taxol for various lengths of time. Equal amounts of protein lysates of the treated cells were immuno-blotted for phosphorylated ERKs (p-ERKs) and total ERKs (a), and phosphorylated MEK (p-MEK) and total MEK (b).

in *BubR1*$^{+/-}$ MEFs. This hyperactivation of ERKs in *BubR1*-deficient cells was manifested as earlier detection of activated forms of ERKs and a greater magnitude and longer persistence of ERK activation than those observed in wild-type MEFs; total ERK levels in these cells were not significantly different (Fig. 1b). Because MEK is the known upstream activator of ERKs, we further analysed activation of MEK in paired MEF cells. Consistently, MEK was activated earlier and at higher magnitude after treatment with nocodazole in *BubR1*$^{+/-}$ MEF cells than in wild-type MEFs; there was no significant difference in total MEK protein level between wild-type MEFs and *BubR1*$^{+/-}$ MEFs before or after nocodazole treatment (Fig. 1b). Furthermore, nocodazole treatment did not alter the level of tyrosine-phosphorylated Cdk1 (Fig. 1b), indicating that short-term treatment was unable to significantly alter the cell population in either cell type. As expected, BubR1 level was lower in *BubR1*$^{+/-}$ MEFs than that in wild-type MEFs (Fig. 1b).

Taxol also exerts microtubule stresses but *via* a different mode of action compared to that of nocodazole (Wilson *et al*. 1999). Treatment with paclitaxel for 5 min significantly activated ERKs and MEK in both wild-type and *BubR1*$^{+/-}$ MEFs, which lasted for at least 10 min before returning to pre-treatment levels (Fig. 2a,b). Despite higher basal levels of phospho-ERKs and phospho-MEK before treatment, which was partly associated with different lines of primary embryonic fibroblast cells used, activation of ERKs and MEK by paclitaxel was significantly more pronounced in *BubR1*$^{+/-}$ cells than in wild-type ones (Fig. 2a,b).

Microtubule disruption results in spindle checkpoint activation and mitotic arrest. To determine whether a defective spindle checkpoint due to *BubR1*-deficiency would compromise cell cycle

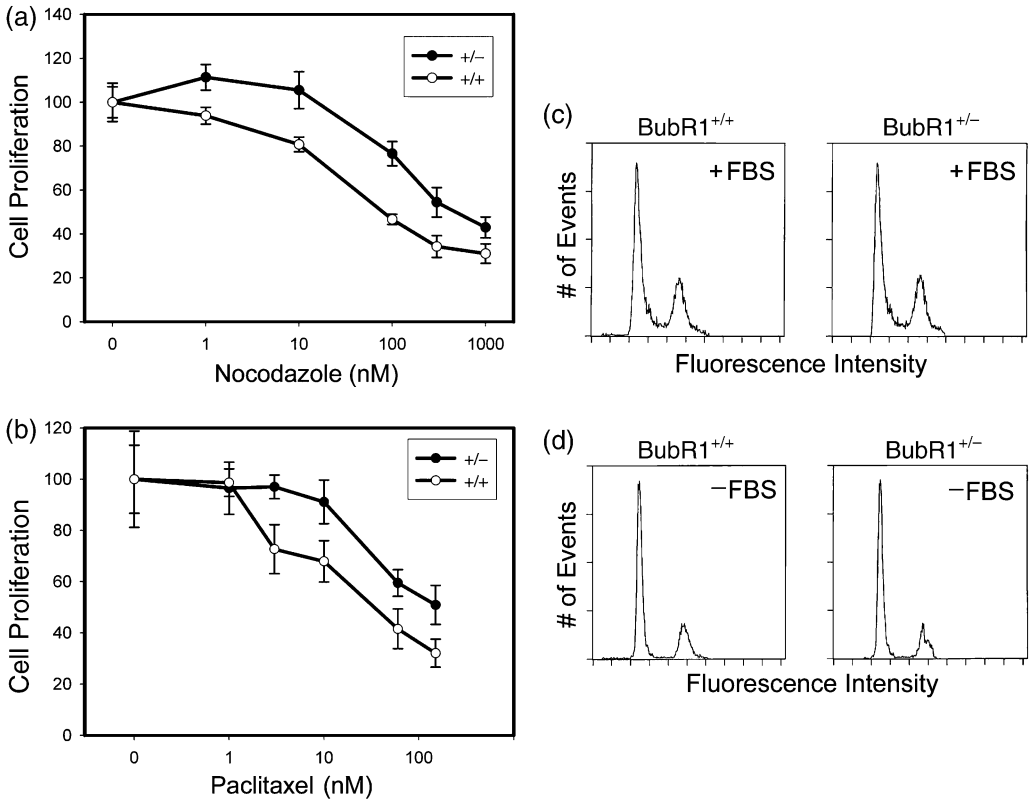

Figure 3. *BubR1*$^{+/-}$ MEF cells survive better than wild-type murine embryonic fibroblast (MEF) cells after microtubule disruption. *BubR1*$^{+/-}$ and wild-type MEF cells cultured in 96-well plates were treated with nocodazole (a) and paclitaxel (b) at various final concentrations. Cell viability was measured using an MTT assay. Each concentration had seven replicates and each experiment was repeated for at least three times. Numbers are presented as means ± SEM. (c) *BubR1*$^{+/-}$ and wild-type MEFs (*BubR1*$^{+/+}$) were analysed for cell cycle distribution via flow cytometry. (d) *BubR1*$^{+/-}$ and wild-type MEFs (*BubR1*$^{+/+}$) were cultured in serum-free medium for 24 h, after which they were analysed for cell cycle distribution using flow cytometry.

arrest or initiate mitotic catastrophe after exposure to microtubule stressors, we analysed the proliferation rate of paired MEF cells treated with nocodazole. We observed that nocodazole suppressed proliferation in both wild-type and *BubR1*$^{+/-}$ MEFs (Fig. 3a); however, *BubR1*$^{+/-}$ MEFs were significantly more resistant to cell population growth inhibition than wild-type MEFs after nocodazole treatment (Fig. 3a). Similar results were also obtained with paired MEFs exposed to paclitaxel. After treatment with low concentrations (< 10 nM) of paclitaxel, cell viability of *BubR1*$^{+/-}$ MEFs was not significantly affected whereas increase in number of wild-type MEFs was impaired (Fig. 3b). There existed little difference in the cell proliferation rate between the wild-type and *BubR1*$^{+/-}$ MEFs; neither population of cells showed enhanced cell death in the absence of serum in the absence of microtubule stresses (Fig. 3c,d). These combined results indicate that cells with *BubR1*-deficiency are more resistant to microtubule stresses, thus conferring a better cell proliferation rate. Consistently, it has been shown that paclitaxel sensitivity of tumour cells is dependent on a functional spindle checkpoint (Sudo *et al*. 2004).

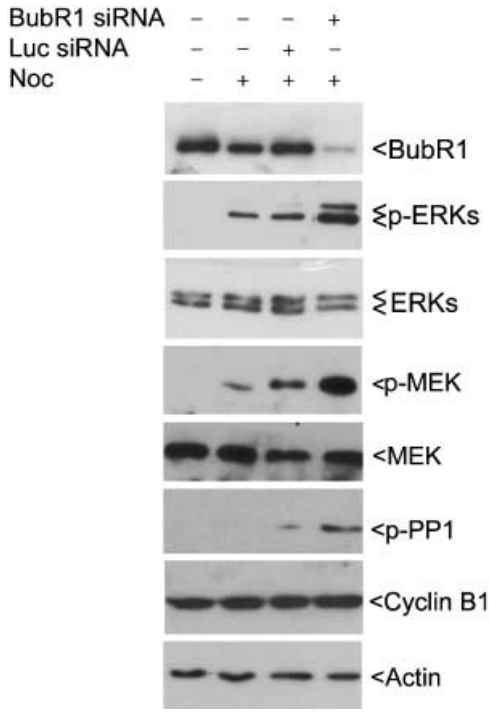

Figure 4. *BubR1* knockdown via RNAi enhanced activation of ERKs and MEK after nocodazole treatment. HeLa cells were transfected with *BubR1* and luciferase siRNAs for 3 days. Transfected, as well as the untransfected control, cells were treated with nocodazole (Noc) for 15 min. Equal amounts of cell lysates were then blotted for *BubR1*, phospho-ERKs, total ERKs, phospho-MEK, total MEK, phospho-PP1 (p-PP1), cyclin B1 and β-actin. Each experiment was repeated for at least three times and similar results were obtained.

To further confirm the role of BubR1 in regulation of the MEK/MAPK pathway, we transfected HeLa cells with specific siRNAs to down-regulate expression of *BubR1*. We observed that *BubR1* knockdown *via* RNAi resulted in enhanced activation of ERKs after exposure to nocodazole (Fig. 4). Enhanced activation of MEK in BubR1 knockdown cells was more prominent compared to those transfected with control siRNA (Fig. 4), thus consistent with the results obtained from *BubR1*-deficient MEF cells. Because protein phosphatase-1 (PP1) is involved in regulating the MEK/MAPK pathway (Manfroid *et al*. 2001), we also blotted lysates with the antibody to the phosphorylated form of PP1 (phosphorylation, which is correlated with its inhibition). We observed that knockdown *BubR1* led to an increase in the level of phosphorylated PP1 (Fig. 4), suggestive of its potential involvement in activation of MEK/MAPKs. *BubR1* knockdown, however, did not significantly change the level of Cyclin B1 (Fig. 4).

As both MEK and ERKs are activated during mitosis and localize to various pieces of mitotic apparatus (Zecevic *et al*. 1998), we re-analysed the intracellular localization of *BubR1*. We found that in addition to the kinetochore localization during early mitosis (Fig. 5a), *BubR1* also exhibited spindle pole-like localization during metaphase (Fig. 5b) and early anaphase (data not shown). Co-staining with γ-tubulin confirmed that *BubR1* localized to spindle poles (Fig. 5c). Consistent with early reports, activated MEK and ERKs were primarily detected at spindle pole regions during metaphase (Fig. 5b,c). Apparent co-localization of *BubR1* with activated ERKs and MEK prompted us to investigate whether these kinases might exist in the same

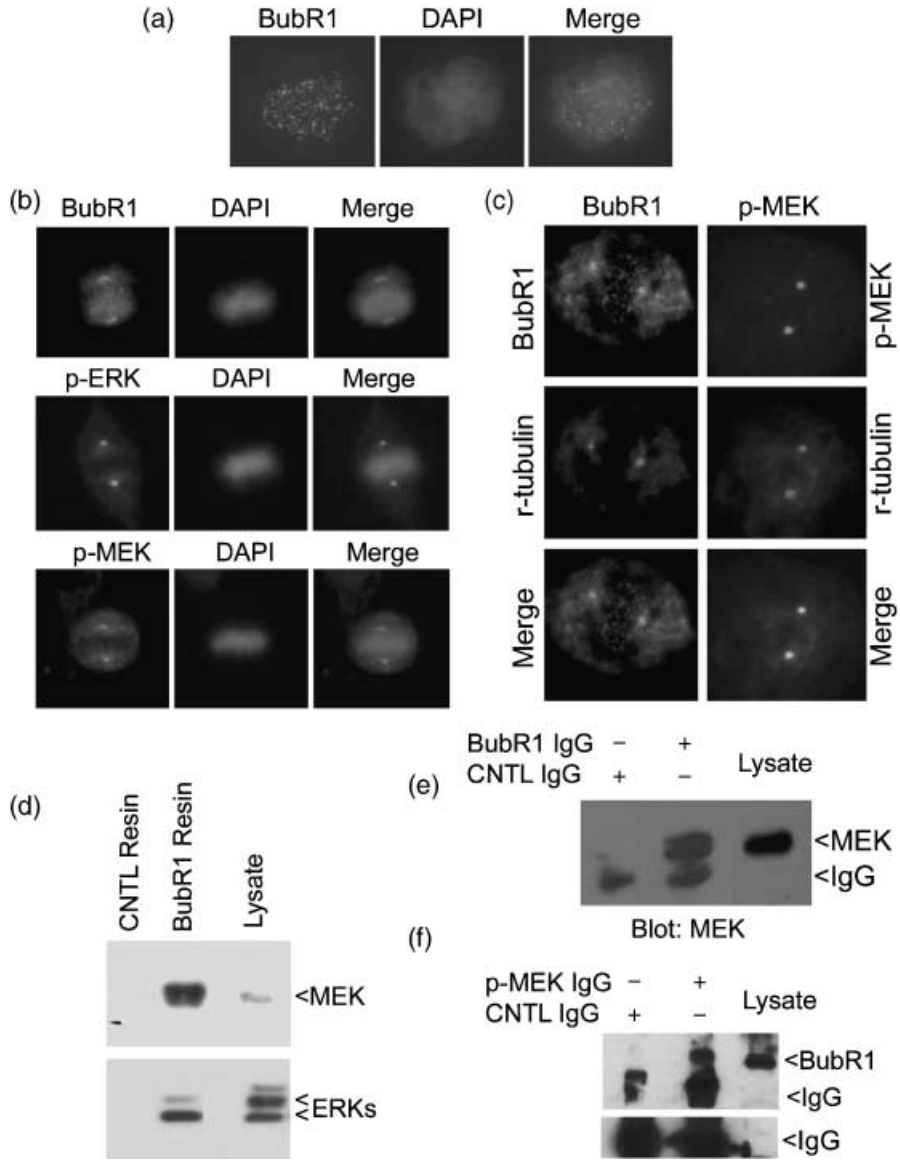

Figure 5. Physical association between *BubR1* and ERKs/MEK. (a) HeLa cells cultured on chamber slides were stained with the antibody to *BubR1* (green). DNA was stained with DAPI (blue). A typical prometaphase cell was shown. (b) HeLa cells were stained with antibodies to BubR1 (green), phospho-ERKs (red) and phospho-MEK (red). Representative metaphase cells were shown. DNA was stained with DAPI. (c) HeLa cells were doubly stained with antibodies to BubR1 and γ-tubulin (left column) or antibodies to phospho-MEK and γ-tubulin (right column). *BubR1* and phospho-MEK were in green and γ-tubulin was in red. (d) His_6-*BubR1* was immobilized onto Ni-NTA resin. His_6-*BubR1* resin and control (CNTL) resin were then incubated with HeLa cell lysates (1 mg each). After thorough washing, proteins specifically interacted with His_6-*BubR1* resin or control resin, as well as HeLa cell lysates (50 μg), were eluted in the SDS-PAGE sample buffer and immunoblotted for MEK and ERKs. (e) HeLa cell lysates were immunoprecipitated with *BubR1* antibody or a control antibody. Immunoprecipitates were blotted for MEK. HeLa cell lysates were also used as a blotting control. (f) HeLa cell lysates were immunoprecipitated with the antibody to phospho-MEK or with a control antibody. Immunoprecipitates were blotted for *BubR1*. HeLa cell lysates were also used as a blotting control. The same blot was stripped and reporbed with an antibody to IgGs, showing the relatively equal amount of loading.

protein complex. Pull-down analysis revealed that His_6-*BubR1* protein immobilized onto Ni-NTA resin was capable of precipitating ERKs and MEK (Fig. 5d). It is interesting to note that ERK2 preferentially pulled down by the *BubR1* resin, whereas no ERK nor MEK signals were precipitated by control resin (Fig. 5d), this is suggestive of physical interaction between ERKs/MEK and *BubR1*. As an alternative approach to confirm the physical interaction between *BubR1* and ERKs/MEK, HeLa cell lysates were immunoprecipitated with the anti-*BubR1* antibody plus with a rabbit control IgG. Immunoprecipitates, along with the cell lysates, were blotted for MEK. We observed that *BubR1* antibody, but not the control antibody, was capable of precipitating MEK signals (Fig. 5e). Similarly, when HeLa cell lysates were immunoprecipitated with the antibody to phospho-MEK, MEK immunoprecipitates, but control immunoprecipitates contained *BubR1* (Fig. 5f). These results thus confirm the physical interaction between *BubR1* and MEK/ERKs.

Impaired spindle checkpoints cause premature separation of sister chromatids. Recent studies show that depletion of Sgo1, a cohesin protector, also results in premature sister chromatid separation and chromosomal missegregation (Wang & Dai 2005; Dai & Wang 2006). To examine whether premature anaphase entry caused by Sgo1 depletion would affect activation of *BubR1*, MEK and ERKs, we transfected HeLa cells with Sgo1 siRNA or luciferase siRNA for 24 h. Transfection of Sgo1 siRNA, but not control siRNA, causes massive mitotic arrest, manifest as appearance of rounded cells that contained condensed but prematurely segregated chromosomes (Wang *et al*. 2006). The rounded cells, as well as the adherent cells, from the culture with Sgo1 depletion were collected and analysed for activation status of *BubR1*, ERKs and MEK. As an additional control, rounded cells from the nocodazole-treated culture were also collected. We observed that whereas *BubR1* was fully activated (phosphorylated) in mitotic cells induced by nocodazole, significant inactivation (dephosphorylated) of *BubR1* occurred in mitotic cells induced by Sgo1 depletion (Fig. 6). Interestingly, no activated ERKs and MEK were detected in nocodazole treated cells, whereas mitotic cells induced by Sgo1 depletion contained a significant amount of phospho-MEK and phospho-ERK2 (Fig. 6). Adherent cells, which had little, if any, activated *BubR1*, contained both phopsho-ERK1 and phospho-ERK2 as well as an elevated level of phospho-MEK; although having no activated *BubR1*, this faction of cells were similar to the rounded cells as the Plk1 level was much higher than in interphase ones; consistently, cell lysates also contained neucleophosmin signals (Fig. 6). Combined, these studies strongly support the notion that activation of ERKs and MEK is inversely correlated with *BubR1* activity during mitosis.

DISCUSSION

Here, we have demonstrated that haplo-insufficiency of *BubR1* facilitates activation of ERKs and MEK by microtubule stressors and that knockdown of *BubR1* via RNAi causes enhanced activation of these kinases too. Several lines of experimental evidence indicate that activation of a spindle checkpoint partly depends on ERKs/MAPKs. Active MAPKs are known to be localized at kinetochores and spindle poles (Zecevic *et al*. 1998). During *Xenopus* oocyte maturation, Bub1, an upstream component of the spindle checkpoint, is activated in a MAPK-dependent manner; moreover, $p90^{Rsk}$, a substrate of MAPKs, is sufficient for activation of Bub1 both *in vivo* and *in vitro* (Schwab *et al*. 2001), suggesting that spindle checkpoint proteins including Bub1 may act downstream of MAPKs and $p90^{Rsk}$. This notion is further supported by the observation that MAPKs contribute to phosphorylation of Bub1 and that inhibition of MAPKs, or a mutation at MAPK phosphorylation consensus sites in Bub1, abolishes phosphorylation and activation of this checkpoint kinase (Chen 2004).

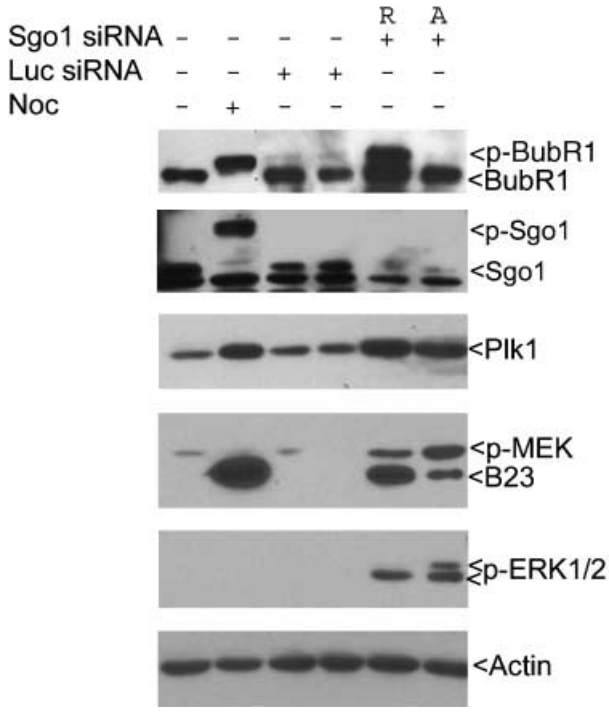

Figure 6. *BubR1* activity was inversely correlated with ERK/MEK activation during mitosis. HeLa cells transfected with Sgo1 siRNA or with luciferase siRNA for 24 h. Rounded-up (lane R) and adherent (lane A) cells from the culture transfected with Sgo1 siRNA were collected separately. In addition, rounded-up cells from the nocodazole-treated group were also collected as control. Equal amounts of cell lysates were blotted for *BubR1*, Sgo1, Plk1, phospho-MEK, phospho-ERKs, B23/nucleophosmin and β-actin.

On the other hand, there also exists some experimental evidence indicating that activation of spindle checkpoint components is independent of the MAPK pathway. For example, spindle defects block both segregation of chromosomes and inactivation of maturation promoting factor during meiosis of mouse oocytes (Brunet *et al*. 2003). Bub1 is localized at kinetochores and is phosphorylated until anaphase entry in both meiotic M phases; the kinetochore localization and phosphorylation of this spindle checkpoint kinase depend on neither MAPK nor Mos, a MEK kinase (Brunet *et al*. 2003). In addition, overexpression of the spindle checkpoint protein Mad2 results in increased phosphorylation of Raf-1, MEK1/2 and Bcl-2 in response to treatment with vincristine (Wang *et al*. 2003), suggesting that Mad2 is capable of modulating the activity of MAPK pathway components. Consistently, premature segregation of chromosomes due to Sgo1 depletion during mitosis causes partial inactivation of *BubR1*, which is correlated with enhanced activation of ERKs and MEK (Fig. 6).

We propose two alternative models, a compensatory model versus a feedback control model, that may help explain the biological significance of our observations. (i) In the compensatory model, *BubR1* and MEK/ERKs act in a cooperative fashion during spindle checkpoint activation. ERKs are known to regulate components involved in spindle checkpoint activation. In fact, ERKs directly phosphorylate, or are involved in regulating phosphorylation of, Bub1, cdc20, CENP-E, upon spindle checkpoint activation (Zecevic *et al*. 1998; Chung & Chen 2003; Chen

2004). Phosphorylated cdc20, along with activated *BubR1*, Mad2 and Bub3, forms mitotic checkpoint complex (MCC) (Sudakin *et al*. 2001), which is essential for the maintenance of functional spindle checkpoint during early mitosis. Thus, the MEK/ERK pathway acts cooperatively with, or in parallel to, spindle checkpoint components, including *BubR1* to ensure full function of the spindle checkpoint. Therefore, it is conceivable that a cell would compensate for the loss of *BubR1*, as in *BubR1*$^{+/-}$ MEFs, by intensifying activation of components (namely, MEK/ERKs) in the other branch of the regulatory network. Given that *BubR1* is involved in chromosome-microtubule attachment, this is especially important when a cell needs to cope with inefficient capturing of kinetochores due to microtubule disruption. This notion is consistent with a recent report that demonstrates that greatly enhanced recruitment of Mad2 to kinetochores occurs in *BubR1*-depleted cells (Lampson & Kapoor 2005). Activity of Cdk1 does not appear to be affected by *BubR1* deficiency in response to microtubule stresses. Phosphorylation of Cdk1 on tyrosine 15, correlating with its inhibition, is not significantly changed in *BubR1*$^{+/-}$ MEFs compared to wild-type MEFs after nocodazole treatment (Fig. 1b); consistently, *BubR1* knockdown does not affect the level of cyclin B in HeLa cells (Fig. 4), suggesting that Cdk1 is not involved in any compensatory functions in *BubR1*-deficient cells.

The feedback control model proposes that *BubR1* is directly involved in regulation of the MEK/ERK signalling pathway. Although at present it remains unclear what the molecular target(s) of *BubR1* is in the MEK/MAPK regulatory circuit, *BubR1* may positively regulate phosphatases such as MKPs and PP1 (or PP2A) that specifically inactivate ERKs and MEK, respectively. Thus, decreased *BubR1* activities would compromise the activation of MKPs or PP1, resulting in an elevated level of MEK and ERKs in *BubR1*-deficient cells. As a precedent, it has been shown that *BubR1* depletion enhances phosphorylation of CENP-A, a potential kinetochore substrate targeted by Aurora kinas (Lampson & Kapoor 2005). Supporting this model, we have observed that PP1 is significantly phosphorylated (inhibited) in nocodazole-treated HeLa cells transfected with *BubR1* siRNA but not control siRNA (Fig. 4). Given that PP1 is involved in regulating the MEK/MAPK pathway (Manfroid *et al*. 2001), our studies may favour the feedback model in which enhanced activation of MEK/ERKs by microtubule stressors in cells haplo-insufficient, or deficient, in *BubR1* is due to suppression of protein phophatase activities involved in negative regulation of MEK/ERKs.

Active MEK and ERKs are easily detectable at spindle poles during prophase and metaphase (Xie *et al*. 2004). It has been established that *BubR1* is predominantly localized at kinetochores during prophase and prometaphase. However, a substantial amount of *BubR1* also exhibits spindle sub-cellular localization during metaphase (Fig. 5b,c) and early anaphase (data not shown), which suggests that spindle poles may be the primary site where *BubR1* and MEK/ERKs may physically and functionally interact. During spindle checkpoint activation, *BubR1* exists as part of MCC, a mitotic checkpoint complex essential for spindle checkpoint activation (Sudakin *et al*. 2001). It would be interesting to examine whether *BubR1* detected at spindle poles is associated with a different molecular complex or whether other MCC components such as Mad2, Bub3 and Cdc20 are also translocated to the spindle poles during metaphase and anaphase when the spindle checkpoint is being inactivated.

ACKNOWLEDGEMENTS

We thank coworkers in the laboratory for various discussions and Lisa Buerle for administrative assistance. This work was supported in part by a core funding from Chinese Academy of

Sciences (CAS), grants of a National Key Program (973) (NO2002CB512805), a One Hundred Talent Grant from CAS to M.X., the E Research Institute of SSMU, the Shanghai Education Commission, and Science and Technology Commission of Shanghai Municipality (04DZ14902), and a grant from the National Institutes of Health (RO1-CA90658) to W.D.

REFERENCES

Arnaoutov A, Dasso M (2003) The Ran GTPase regulates kinetochore function. *Dev. Cell* **5**, 99–111.

Bharadwaj R, Yu H (2004) The spindle checkpoint, aneuploidy, and cancer. *Oncogene* **23**, 2016–2027.

Brunet S, Pahlavan G, Taylor S, Maro B (2003) Functionality of the spindle checkpoint during the first meiotic division of mammalian oocytes. *Reproduction* **126**, 443–450.

Cahill DP, Lengauer C, Yu J, Riggins GJ, Willson JK, Markowitz SD, Kinzler KW, Vogelstein B (1998) Mutations of mitotic checkpoint genes in human cancers. *Nature* **392**, 300–303.

Castro A, Peter M, Lorca T, Mandart E (2001) c-Mos and cyclin B/cdc2 connections during *Xenopus* oocyte maturation. *Biol. Cell* **93**, 15–25.

Chan GK, Jablonski SA, Sudakin V, Hittle JC, Yen TJ (1999) Human *BubR1* is a mitotic checkpoint kinase that monitors CENP-E functions at kinetochores and binds the cyclosome/APC. *J. Cell Biol*. **146**, 941–954.

Chen RH (2004) Phosphorylation and activation of Bub1 on unattached chromosomes facilitate the spindle checkpoint. *EMBO J*. **23**, 3113–3121.

Chung E, Chen RH (2003) Phosphorylation of Cdc20 is required for its inhibition by the spindle checkpoint. *Nat. Cell Biol*. **5**, 748–753.

Dai W, Wang X (2006) The Yin and Yang of centromeric cohesion of sister chromatids: mitotic kinases meet protein phosphatase 2A. *Cell Div*. **1**, 9.

Dai W, Wang Q, Liu T, Swamy M, Fang Y, Xie S, Mahmood R, Yang YM, Xu M, Rao CV (2004) Slippage of mitotic arrest and enhanced tumor development in mice with *BubR1* haploinsufficiency. *Cancer Res*. **64**, 440–445.

Hanks S, Coleman K, Reid S, Plaja A, Firth H, Fitzpatrick D, Kidd A, Mehes K, Nash R, Robin N, Shannon N, Tolmie J, Swansbury J, Irrthum A, Douglas J, Rahman N (2004) Constitutional aneuploidy and cancer predisposition caused by biallelic mutations in Bub1B. *Nat. Genet*. **36**, 1159–1161.

Lampson MA, Kapoor TM (2005) The human mitotic checkpoint protein *BubR1* regulates chromosome-spindle attachments. *Nat. Cell Biol*. **7**, 93–98.

Lengauer C (2003) Cancer. An unstable liaison. *Science* **300**, 442–443.

Lengauer C, Kinzler KW, Vogelstein B (1998) Genetic instabilities in human cancers. *Nature* **396**, 643–649.

Manfroid I, Martial JA, Muller M (2001) Inhibition of protein phosphatase PP1 in GH3B6, but not in GH3 cells, activates the MEK/ERK/c-fos pathway and the human prolactin promoter, involving the coactivator CPB/p300. *Mol. Endocrinol*. **15**, 625–637.

Minshull J, Sun H, Tonks NK, Murray AW (1994) A MAP kinase-dependent spindle assembly checkpoint in *Xenopus* egg extracts. *Cell* **79**, 475–486.

Ouyang B, Pan H, Lu L, Li J, Stambrook P, Li B, Dai W (1997) Human Prk is a conserved protein serine/threonine kinase involved in regulating M phase functions. *J. Biol. Chem*. **272**, 28646–28651.

Rao CV, Yang YM, Swamy MV, Liu T, Fang Y, Mahmood R, Jhanwar-Uniyal M, Dai W (2005) Colonic tumorigenesis in *BubR1*$^{+/-}$ ApcMin/+ compound mutant mice is linked to premature separation of sister chromatids and enhanced genomic instability. *Proc. Natl. Acad. Sci. USA* **102**, 4365–4370.

Reszka AA, Seger R, Diltz CD, Krebs EG, Fischer EH (1995) Association of mitogen-activated protein kinase with the microtubule cytoskeleton. *Proc. Natl. Acad. Sci. USA* **92**, 8881–8885.

Roovers K, Assoian RK (2000) Integrating the MAP kinase signal into the G_1 phase cell cycle machinery. *Bioessays* **22**, 818–826.

Schwab MS, Roberts BT, Gross SD, Tunquist BJ, Taieb FE, Lewellyn AL, Maller JL (2001) Bub1 is activated by the protein kinase p90 (Rsk) during *Xenopus* oocyte maturation. *Curr. Biol*. **11**, 141–150.

Shapiro PS, Vaisberg E, Hunt AJ, Tolwinski NS, Whalen AM, McIntosh JR, Ahn NG (1998) Activation of the MKK/ERK pathway during somatic cell mitosis: direct interactions of active ERK with kinetochores and regulation of the mitotic 3F3/2 phosphoantigen. *J. Cell Biol*. **142**, 1533–1545.

Sudakin V, Chan GK, Yen TJ (2001) Checkpoint inhibition of the APC/C in HeLa cells is mediated by a complex of BubR1, Bub3, cdc20, and Mad2. *J. Cell Biol*. **154**, 925–936.

Sudo T, Nitta M, Saya H, Ueno NT (2004) Dependence of paclitaxel sensitivity on a functional spindle assembly checkpoint. *Cancer Res*. **64**, 2502–2508.

Tong C, Fan HY, Chen DY, Song XF, Schatten H, Sun QY (2003) Effects of MEK inhibitor U0126 on meiotic progression in mouse oocytes: microtuble organization, asymmetric division and metaphase II arrest. *Cell Res*. **13**, 375–383.

Verlhac MH, Lefebvre C, Kubiak JZ, Umbhauer M, Rassinier P, Colledge W, Maro B (2000) Mos activates MAP kinase in mouse oocytes through two opposite pathways. *EMBO J*. **19**, 6065–6074.

Wang X, Dai W (2005) Shugoshin, a guardian for sister chromatid segregation. *Exp. Cell Res*. **310**, 1–9.

Wang X, Jin DY, Wong HL, Feng H, Wong YC, Tsao SW (2003) Mad2-induced sensitization to vincristine is associated with mitotic arrest and Raf/Bcl-2 phosphorylation in nasopharyngeal carcinoma cells. *Oncogene* **22**, 109–116.

Wang Q, Xie S, Chen J, Fukasawa K, Naik U, Traganos F, Darzynkiewicz Z, Jhanwar-Uniyal M, Dai W (2002) Cell cycle arrest and apoptosis induced by human Polo-like kinase 3 is mediated through perturbation of microtubule integrity. *Mol. Cell Biol*. **22**, 3450–3459.

Wang X, Yang Y, Dai W (2006) Differential subcellular localizations of two human Sgo1 isoforms: implications in regulation of sister chromatid cohesion and microtubule dynamics. *Cell Cycle* **5**, 635–640.

Wilson L, Panda D, Jordan MA (1999) Modulation of microtubule dynamics by drugs: a paradigm for the actions of cellular regulators. *Cell Struct. Funct*. **24**, 329–335.

Xie S, Wang Q, Ruan Q, Liu T, Jhanwar-Uniyal M, Guan K, Dai W (2004) MEK1-induced Golgi dynamics during cell cycle progression is partly mediated by Polo-like kinase-3. *Oncogene* **23**, 3822–3829.

Zecevic M, Catling AD, Eblen ST, Renzi L, Hittle JC, Yen TJ, Gorbsky GJ, Weber MJ (1998) Active MAP kinase in mitosis: localization at kinetochores and association with the motor protein CENP-E. *J. Cell Biol*. **142**, 1547–1558.

